QUANTIFICATION OF NOTCH-TYPE DAMAGE IN A TWO-STOREY FRAMED STRUCTURE UTILISING FREQUENCY RESPONSE FUNCTIONS AND ARTIFICIAL NEURAL NETWORKS

U. Dackermann
University of Technology Sydney, Centre for Built Infrastructure Research, AUSTRALIA
udacker@gmail.com

J. Li
University of Technology Sydney, Centre for Built Infrastructure Research, AUSTRALIA
jianchun.li@uts.edu.au

B. Samali
University of Technology Sydney, Centre for Built Infrastructure Research, AUSTRALIA
bijan.samali@uts.edu.au

Abstract

For civil engineering structures damage will inevitably occur and continuously accumulate during their service life. As damage develops, the physical properties of the structure change and in turn, its dynamic characteristics alter. It is, therefore, feasible to utilise measured dynamic quantities such as time histories, frequency response functions (FRFs) and modal parameters from structural vibration to identify damage characteristics.

This paper presents a damage identification method that utilises FRF data to determine severities of notch-type damage in a two-storey framed structure. The proposed method utilises artificial neural networks (ANNs) to map changes in FRFs to damage severities. To obtain suitable patterns for ANN inputs, the size of the measured FRF data is reduced by adopting principal component analysis (PCA) techniques. A hierarchy of neural network ensembles is created to take advantage of individual characteristics of data recorded from different sensor locations. The method is verified by a laboratory and a numerical two-storey framed structure, which is each inflicted with a number of single notch-type damage scenarios of different locations and severities. To simulate field-testing conditions, numerically simulated data is polluted with white Gaussian noise of up to 10% noise-to-signal-ratio.

Introduction

Vibration-based damage identification methods are global non-destructive techniques used to investigate critical changes in dynamic parameters in order to prevent unexpected catastrophic failures of structures. To date, intensive research has been undertaken in the field of vibration-based damage detection and so far most developed methods use modal data such as natural frequencies and mode shapes to identify damage. In recent years, however, there is an emerging trend of using directly measured FRF data to detect structural damage (Huynh, He et al. 2005). Utilising FRFs to form a damage indicator may have several advantages: FRFs are usually the most compact form of data obtained from vibrational testing, and hence, they provide an abundance of information on a structure's dynamic behaviour. Unlike modal parameter methods, FRF-based damage detection techniques do not require experimental modal analysis, which involves intensive labour and is very susceptible to human error.

In structural damage identification, the primary sources of difficulties include measurement noise, modeling error, uncertainty of ambient conditions and incompleteness of measured data. Whilst most of developed damage detection methods work successfully when noise-free simulated data are used, presence of the uncertainties due to modeling and measurement errors causes many of the methods to fail (Wang, Ni et al. 2000). It is generally acknowledged that ANNs tend to be robust in the presence of noise and can distinguish between these random errors and the desired systematic outputs (Levin and Lieven

1998). Using a combination of FRFs and ANNs for structural damage identification is therefore a promising field of research and some successful results have already been obtained (Marwala and Hunt 1999; Zang and Imregun 2001; Ni, Zhou et al. 2006). A challenge in utilising FRFs as inputs for ANNs, however, is the large size of the FRF data. Utilising full-size FRFs in neural networks will cause problems in training convergence and computational efficiency. Principal component analysis (PCA) is a statistical technique that is known for its capability of reducing the dimension of data as well as its ability of reducing the influence of uncertainties by filtering unrepeatable random features. By projecting data onto the most important principal components, its size can greatly be reduced without significantly affecting the data. Using PCA in combination with FRFs and ANNs can overcome the size issue of FRF data, and in addition, reduce the effects of measurement noise and other random uncertainties.

In this paper, a damage identification method is presented that utilises damage fingerprints embedded in FRF data to identify severities of notch-type damage in laboratory and numerical models of a two-storey framed structure. The proposed method uses ANNs to analyse pattern changes in residual FRFs, which are differences in FRF data between the undamaged and damaged structures, to identify defects. To obtain suitable input data for network training and to filter uncertainties such as measurement noise, the residual FRFs are compressed to a few principal components using PCA techniques. A hierarchy of neural network ensembles is utilised to take advantage of different characteristics obtained from individual measurements from various sensor locations.

The Two-Storey Framed Structure

A two-storey framed structure was utilised to test the proposed damage identification method. First, a laboratory model of the structure was manufactured and tested in the Structures Laboratory of the University of Technology Sydney (UTS) and then the experimental structure was numerically modelled and analysed with the finite element software ANSYS. The two-storey framed structure was made of steel and consisted of two columns, two crossbeams and four joint elements.

Laboratory Model

For the laboratory model of the test structure, the two columns were made of flat steel with a cross-section of 65 mm × 5.5 mm and a height of 1600 mm. For the two crossbeams, the main body consisted of a box section of 150 mm × 50 mm with a wall thickness of 3 mm. The crossbeams were located 700 mm and 1400 mm above the steel base connection, respectively and there was a spacing of 700 mm between the steel base connection and the lower beam, and between the two crossbeams. The steel had a modulus of elasticity of $200{,}000 \times 10^6$ N/m^2, the Poisson's ratio was 0.3 and the density was 7,850 kg/m^3. A photo of the laboratory model with indications of the main structural elements and relevant dimensions is displayed in Figure 1 (a).

Single notch-type damage of different severities was inflicted to one of the columns. Two damage sites were considered, these were locations '1' and '3' of Figure 1 (b), which are 350 mm and 1,050 mm above the steel base connection, respectively. These two locations are the mid-spans of the upper and the lower column halves. At each location, damage of three severities was gradually inflicted to the column. The three levels of damage severities, termed light ('L'), medium ('M') and severe ('S'), were introduced corresponding to a section loss of 4 mm in notch width and 16.25 mm, 21.7 mm and 32.5 mm in notch depth, respectively. The inflicted section losses correspond to a cross-section loss of the second moment of area, I, of 25%, 33.33% and 50%, respectively. Damage of all three severities is depicted in Figure 2. All investigated damage scenarios are listed in Table 1.

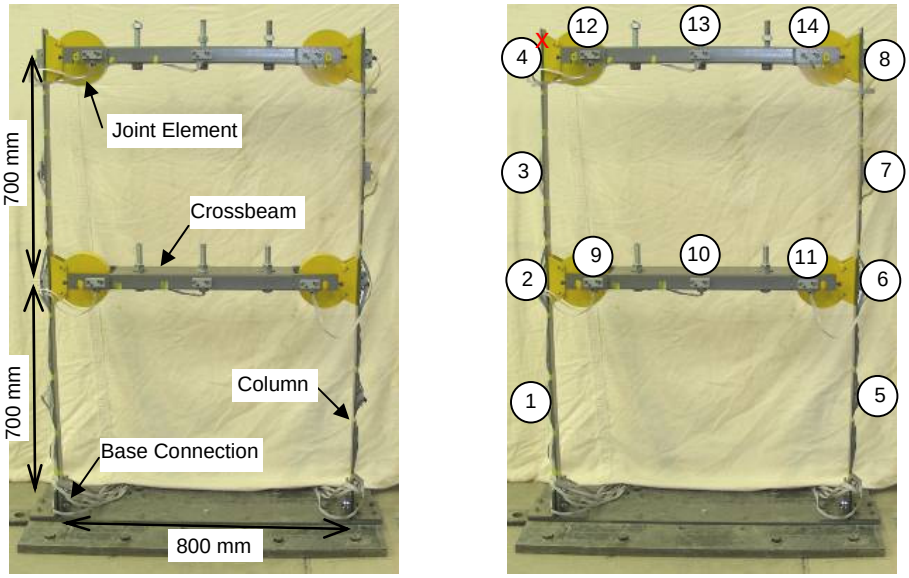

(a) (b)

Figure 1 Laboratory two-storey framed structure indicated with (a) main structural elements and dimensions, and (b) accelerometer locations and hammer impact point.

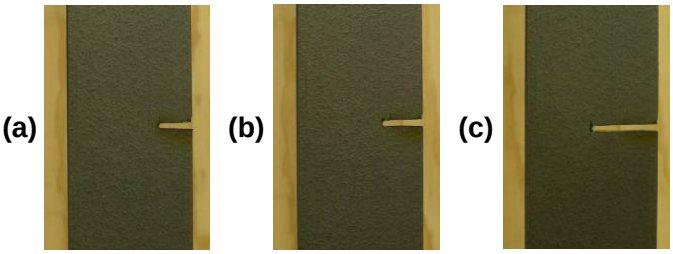

Figure 2 (a) Light, (b) medium and (c) severe size damage.

Table 1 Damage scenarios.

Damage scenario	Damage location	Damage severity	Loss of I
'1L'	'1'	'L'	25%
'1M'	'1'	'M'	33.33%
'1S'	'1'	'S'	50%
'3L'	'3'	'L'	25%
'3M'	'3'	'M'	33.33%
'3S'	'3'	'S'	50%

The dynamic properties of the laboratory two-storey framed structure were determined using modal testing and experimental modal analysis (MT&EMA) techniques. In modal testing, the structure was excited with a modally tuned impact hammer. The reference point for the hammer was located at the upper end of the column indicated with a red cross in Figure 1 (b). The hammer strike was executed in the horizontal direction resulting in a lateral excitation of the structure. The responses of the structure were measured by 14 accelerometers, which were mounted to the columns and the crossbeams. The locations of the sensors are indicated in Figure 1 (b) by the numbers '1' to '14'. The accelerometers at locations '1' to '8' were mounted on the centreline of the columns and were set up to measure horizontal accelerations. As the crossbeams experienced negligible horizontal deformation, the accelerometers of locations '9' to '14' were mounted to one side of the crossbeams and measured acceleration in the vertical direction. The accelerometers used for the testing were low cost dual-axis piezoresistive accelerometers of model ADXL320 having a bandwidth of 0.5 Hz to 2.5 kHz. The accelerometers were supplied with a 5 V DC power excitation measuring a range of ±5 g. The data acquisition system used was an Iotech Daqbook 260 equipped with 2×16 input channels. In experimental modal analysis, the acquired signals from the impact hammer and the 14 accelerometers were analysed and the modal parameters of the structure determined. For each test, the sampling rate was set to 1,000 Hz capturing a frequency range of 0 - 500 Hz and 8,192 data points, thus giving a frequency resolution of 0.061 Hz per data point. FRF data were

determined and the natural frequencies, damping ratios and corresponding mode shapes were extracted using the modal analysis module of the LMS CADA-X software (CADA-X 1996). As each damage scenario was tested 5 times, a total of 35 FRF recordings for the six different damage cases and the undamaged state of the structure were generated.

Numerical Model

The finite element model of the two-storey framed structure was created with ANSYS Workbench (ANSYS Inc 2007). A picture of the meshed structure in front view is illustrated in Figure 3 (a). For the numerical structure, notch-type damage was inflicted at six different locations, i.e. locations '1a', '1b' and '1c' of the lower column half and locations '3a', '3b', and '3c' of the upper column half (see Figure 3 (b)). Locations '1a' and '3a' are at the midspans of the column halves and correspond to locations '1' and '3' of the laboratory structure. At each of the six locations, damage of three severities ('L', 'M' and 'S') was modelled, resulting in a total of 18 different damage cases. The damage severities are the same as for the laboratory model having a notch width of 4 mm and a notch depth of 16.25 mm, 21.7 mm and 32.5 mm, respectively, for the three severities 'L', 'M' and 'S'. Damage of light and medium size is illustrated in Figure 3 (c) and (d).

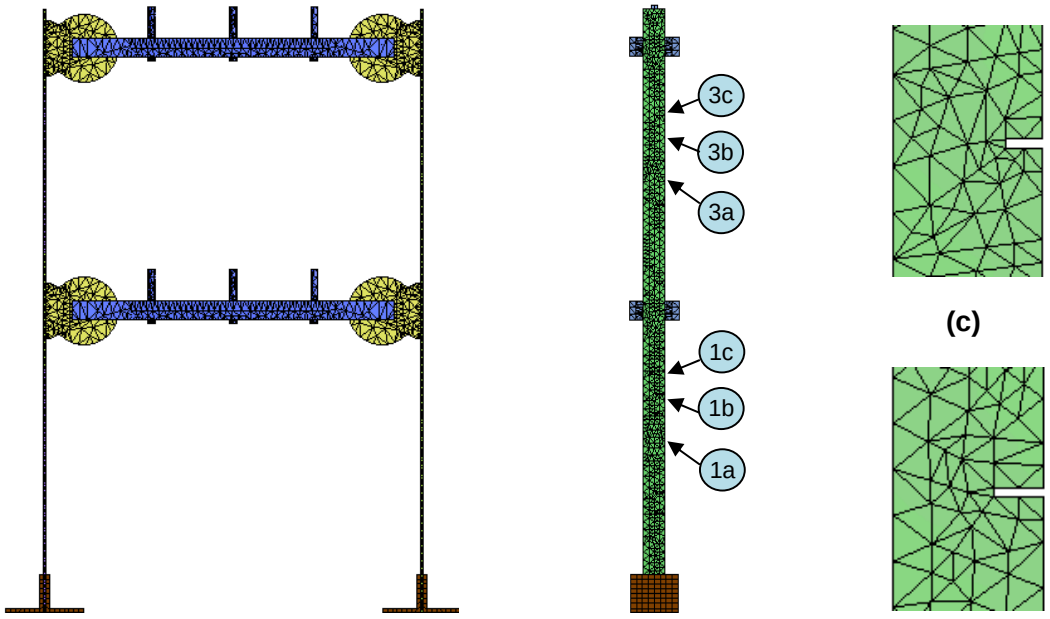

Figure 3 (a) Numerical model of the structure (front view); (b) indications of numerical damage locations (side view); and (c) damage of light and (d) medium size.

To determine the dynamic properties of the numerical models, transient analysis was performed in ANSYS Classic (ANSYS Inc 2007). Therefore, an impact force of 500 N was applied at the reference point of the hammer and the response time histories of the structure were sampled at locations '1' to '14', which were the sensor locations in the experimental testing (see Figure 1 (b). The response of the structure was recorded for 16.385 s in integration time steps of 0.001 s, resembling the sampling rate from the experimental testing. At locations '1' to '8' (on the columns), the time histories were recorded in the horizontal direction, and at locations '9' to '14' (on the crossbeams), the time history data were sampled in the vertical direction.

To simulate real testing conditions, the recorded time history data were polluted with white Gaussian noise of four intensities (1%, 2%, 5% and 10% noise-to-signal-ratio). For each level of noise pollution, five sets of noise-contaminated data were generated to simulate five repeated tests. Next, FRFs were calculated that captured a frequency range of 0−500 Hz and comprised 8,192 spectral lines, resulting in a frequency resolution of 0.061 Hz per data point, which equals the resolution obtained from the experimental testing.

Dynamic Characteristics of Two-Storey Framed Structure

For the laboratory and numerical models of the two-storey framed structure, the dynamic characteristics (i.e. FRFs, natural frequencies and mode shapes) were determined for the undamaged and the damaged states of the structure. For the undamaged laboratory structure, the determined horizontal FRF summation function (resulting from the summation of the FRFs of accelerometers at locations '1' to '8', which capture horizontal accelerations) is displayed in Figure 4 (a). From the illustrated FRF, the frequency peaks of the first seven flexural modes are clearly visible and are labelled with arrows. From mode shape diagrams of these modes, it was found that modes 1 and 2 are global modes and modes 3 to 7 are local modes. Whereas mode 1 and mode 2 describe the shapes of the first and second flexural modes of a cantilever, respectively, modes 3 to 7 show different combinations of local column deformations, which all describe shapes similar to the first flexural mode of a beam.

For the different damage states of the two-storey framed structure, some changes to the dynamic properties, e.g. FRFs, natural frequencies and mode shapes, did occur. As an example, Figure 4 (b) displays the horizontal FRF summation functions of the laboratory structure in its undamaged state (intact) and with damage at location '3' with severities 'L', 'M' and 'S'. From the FRFs, it can be seen that for different damage scenarios individual changes of the FRFs do occur, i.e. changes in amplitude, shape and position of the frequency peaks. These changes in FRF data, which represent unique damage fingerprints, form the basis of the proposed damage identification method.

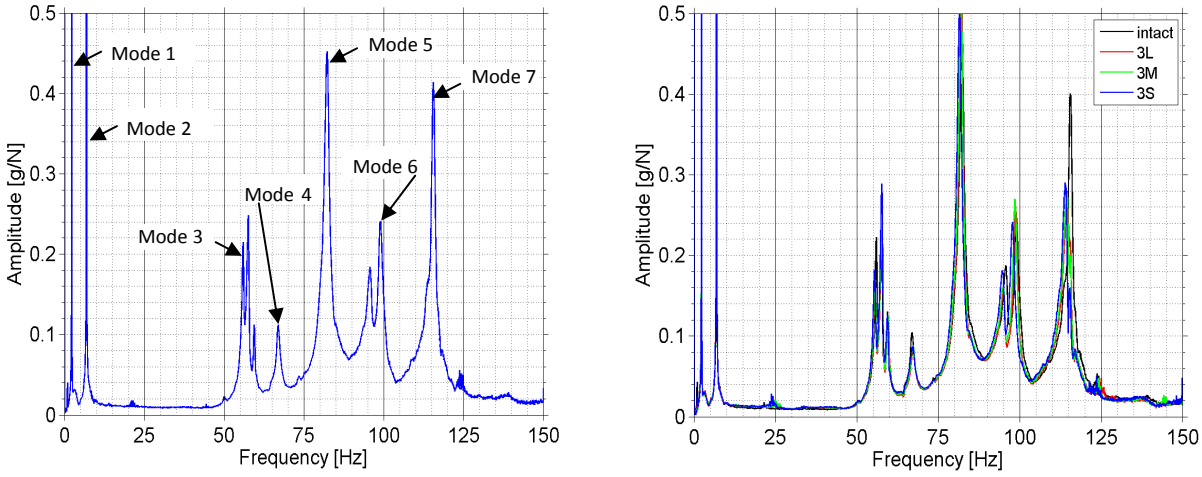

Figure 4 Horizontal FRF summation functions of (a) undamaged state and (b) undamaged and different damaged states of laboratory model.

Damage Identification Procedure

Methodology

This paper presents a vibration-based damage detection method that identifies severity of single damage cases in a two-storey framed structure from damage fingerprints in FRF data. ANNs are utilised to map pattern changes in FRFs to damage characteristics. To enhance damage fingerprints in FRF data, residual FRFs, which are differences in FRF data from the undamaged and the damaged structure, are used to indicate damage. To obtain suitable input data for network training, residual FRFs are compressed to a few principal components adopting PCA techniques. A hierarchy of neural network ensembles is utilised to respect and take advantage of different characteristics obtained by individual measurements from various sensor locations. To test the method, it is applied to laboratory and numerical models of a two-storey framed structure. For the numerical models, white Gaussian noise is added to the generated data in order to simulate field-testing conditions.

In the proposed damage identification procedure, firstly, time history data are obtained from the laboratory and numerical two-storey framed structure at different measurement locations by means of experimental testing or finite element analysis, respectively. That is, impact hammer testing is conducted for the laboratory structure, and transient analysis with subsequent noise contamination is performed for the numerical structure. Secondly, FRFs are calculated from the time history data and residual FRFs are obtained by computing FRF differences between the undamaged and the damaged structures. Thirdly, by adopting PCA techniques, the residual FRFs are compressed and the most important principal components identified. Fourthly, sets of individual neural networks are trained with PCA-compressed residual FRFs of different measurement locations to identify location and severity of the damage. Finally, a neural network ensemble fuses the outcomes of the individual networks and an overall damage prediction is obtained. A flow-chart of the damage identification procedure of the numerical two-storey framed structure is presented in Figure 5.

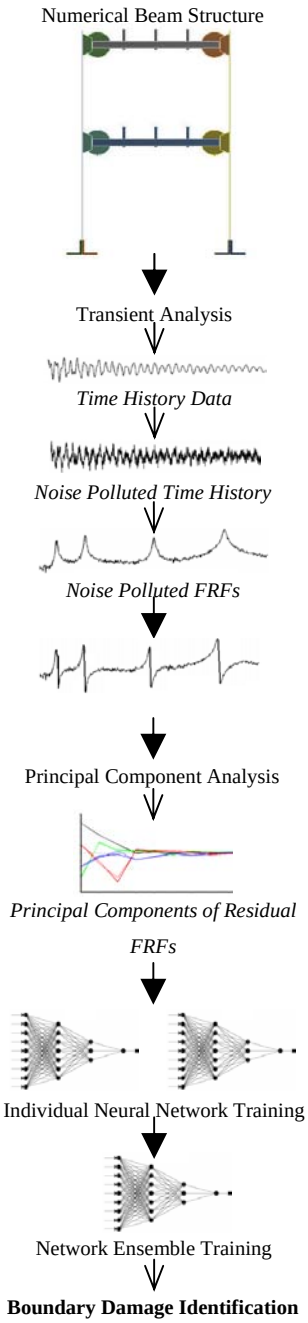

Figure 5 Flow-chart of damage identification procedure.

Residual FRFs

Damage caused changes in FRF data such as shifting of frequency peaks and changes of FRF amplitudes (as presented above). To enhance these damage fingerprints in FRF data, in the proposed method, residual FRFs were used as damage indicator to determine severity of damage. Residual FRF data are defined in as:

$$ResH(\omega) = H_d(\omega) - H_{und}(\omega) \quad (1)$$

where $H_d(\omega)$ is the FRF data from the damaged structure and $H_{und}(\omega)$ is the FRF data from the undamaged structure.

For the laboratory two-storey framed structure, Figure 6 (a) illustrates residual FRFs (from the horizontal FRF summation functions) for damage at location '3' with the severities 'L', 'M' and 'S'. From the figure, it is noted that residual FRF values closest to the frequency peaks were most affected by the damage. A close-up of FRF changes in the vicinity of the frequency peak of mode 5 are displayed in Figure 6 (b). From this graph, it is observed that for different damage severities explicit amplitude changes have occurred (the larger the damage extend the bigger the amplitude change). These unique patterns in residual FRFs were used in the presented algorithm to quantify damage.

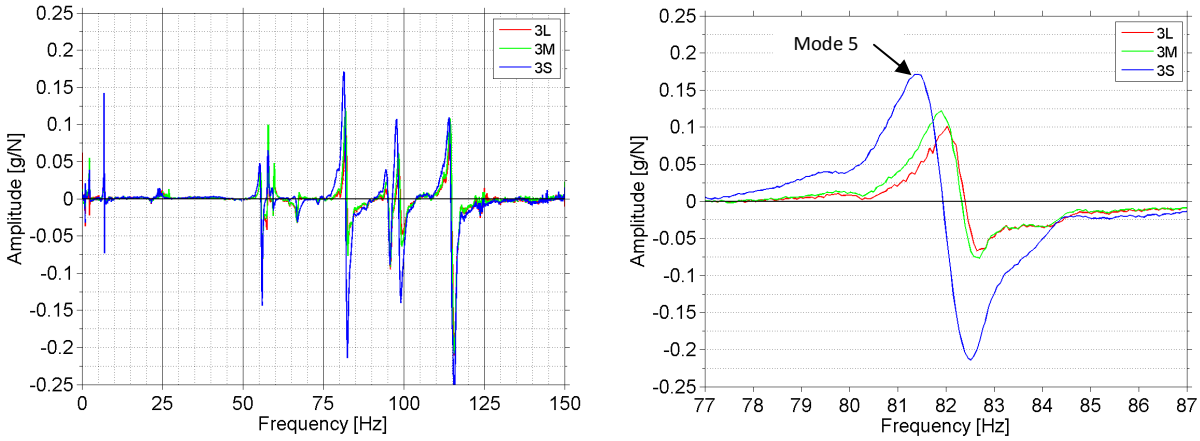

Figure 6 Residual FRFs (from horizontal FRF summation functions) of laboratory structure with light, medium and severe damage at location '3' of (a) frequency range from 0 to 150 Hz and (b) close-up of the frequency peak of mode 5.

Principal Components of Residual FRFs

To produce damage indices that are suitable for neural network training, the size of the residual FRFs must be greatly reduced. A full-size residual FRF, which covers a frequency range of 0 to 150 Hz (capturing the first seven flexural modes), contains 2,458 spectral lines. This corresponds to 2,458 input nodes in the neural network. Such large numbers of input points cause severe problems in training convergence in addition to computational inefficiency. Therefore, PCA, which is one of the most powerful statistical multivariate data analysis techniques for achieving dimensionality reduction, was used to reduce the size of the residual FRF data.

For data reduction of the residual FRFs, two matrices containing the data of all available residual FRFs of the numerical and laboratory structure, respectively, were formed and projected onto their PCs. A plot of the determined individual and the cumulative contribution of the first 100 PCs of the residual FRFs of the numerical structure with 1% noise pollution (from horizontal FRF summation function) is shown in Figure 7 (a). It was found that the first 10 PCs account for 71.8% contribution of the original data. The individual contribution percentage of each of the first five PCs was 22.5%, 10.4%, 8.1%, 7.8% and 4.6%.

To determine the optimal number of PCs that contain sufficient data for damage identification, a study on the sensitivity of the PCs to damage was undertaken. As an example, Figure 7 (b) illustrates the first 17 PCs of residual FRFs of different damage scenarios (damage at location '3a' of severities 'L', 'M' and 'S') from numerical simulations polluted with 1% noise. For each depicted damage scenario, three different data sets, each polluted with random numbers of 1% white Gaussian noise, are displayed. From the figure, it can be seen that the first ten PCs show clear distinguishable patterns for the various damage scenarios. From the 11th component onwards, PC values are smaller (in absolute values) and very similar for all damage scenarios indicating their insignificant contribution for the damage cases investigated.

Further, the three data sets of each damage scenario group together, and thus they are represented by the same PCs. Such clustering behaviour and the distinct patterns of the different damage cases are ideal conditions for neural-network-based pattern recognition. From these findings, it was concluded that it was sufficient to use the first 10 PCs as input parameters for neural network training.

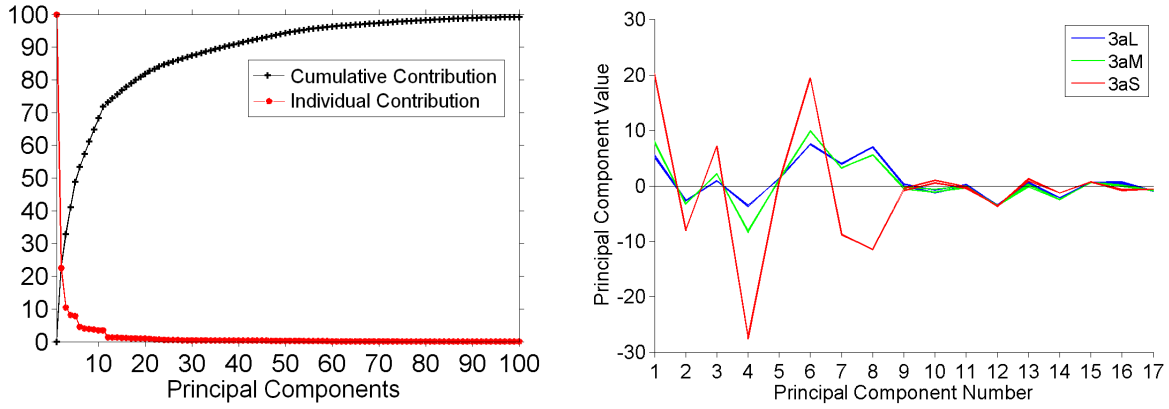

Figure 7 (a) PC contributions of the first 100 PCs of all residual FRFs (from FRF summation function location '5') and (b) first 17 PCs of residual FRFs (from measurement location '5') of damage cases '3aL', '3aM' and '3aS' of numerical data polluted with 1% white Gaussian noise.

Design of Artificial Neural Networks

To identify damage severities, a number of multi-layer back propagation neural networks were created. The design and operation of all created neural networks was performed with the software Alyuda NeuroIntelligence version 2.2 from Alyuda Research Inc (Alyuda Research Inc 2006). For the laboratory and numerical structure, 16 individual networks and one network ensemble were designed. The individual networks were trained with PCs of residual FRFs obtained from modal testing and transient analysis, respectively. Out of the 16 individual networks, 14 were trained with data obtained from the 14 sensor locations and two were trained with data derived from horizontal and vertical summation FRFs (which were obtained by summing the FRFs of horizontal accelerations of measurement locations '1' to '8' and of vertical accelerations of measurement locations '9' to '14' , respectively). The network ensemble was trained with the outcomes of the 14 individual sensor networks. The outcomes of the horizontal and vertical summation FRF networks were compared against the results of the neural network ensemble to demonstrate advantage of the network ensemble.

To avoid overfitting of the networks, the input data was separated into training, validation and testing sets. For each damage scenario, five sets of FRF measurements were available for the laboratory and the numerical two-storey framed structure. (For the laboratory structure, each state was tested five times; and for the numerical model, acceleration data was polluted with five sets of different noise signals for each noise pollution level.) To calculate residual FRFs, the five samples of FRF data from the damaged states were correlated to each of the five samples of FRFs obtained from the undamaged state. Therefore, a total of 25 residual FRFs (and consequently 25 neural network input samples) were available for each damage scenario. The division of the data into sets for training ('train'), validation ('val') and testing ('test') was accomplished by a partitioning system termed 'chessboard selection', which is illustrated in Table 2. Here, data of the three categories ('train', 'val' and 'test') were selected along a diagonal line in order to provide a diverse range for each data set. Thereby, the 25 available residual FRFs of each damage

scenario were separated into 15 training, 5 validation and 5 testing samples. The total number of input samples of the training, validation and testing sets for the laboratory and numerical structure are listed in Table 3.

Table 2 Data partitioning with chessboard system.

		Undamaged data				
		U1	U2	U3	U4	U5
Damaged data	D1	Train	Val	Train	Train	Test
	D2	Test	Train	Val	Train	Train
	D3	Train	Test	Train	Val	Train
	D4	Train	Train	Test	Train	Val
	D5	Val	Train	Train	Test	Train

Table 3 Training, validation and testing partitioning of data obtained from the laboratory and numerical structure.

	Set	Samples	Remarks
Laboratory Structure	Training	90	6 damage scenarios (2 locations × 3 severities) × 15 samples
	Validation	30	18 damage scenarios (2 locations × 3 severities) × 5 samples
	Testing	30	6 damage scenarios (2 locations × 3 severities) × 5 samples
Numerical Structure	Training	1080	18 damage scenarios (6 locations × 3 severities) × 15 samples × 4 noise levels
	Validation	360	18 damage scenarios (6 locations × 3 severities) × 5 samples × 4 noise levels
	Testing	360	18 damage scenarios (6 locations × 3 severities) × 5 samples × 4 noise levels

The transfer functions used for all networks were hyperbolic tangent sigmoid functions. As convergence algorithm, the online backpropagation function was used for all networks trained with data of the laboratory structure (as well as the network ensembles trained with numerical data) and the conjugate gradient descent function was employed for all individual networks of the numerical structure. All individual neural networks were designed with an input layer of 10 nodes representing the number of the selected PCs; four hidden layers of 8, 6, 4 and 2 nodes and one single node output layer estimating the severity of the damage. The network ensemble comprised of 14 input nodes, which were the outputs of the 14 individual networks; five hidden layers also consisting of 10, 8, 6, 4 and 2 nodes and one output node predicting the damage severity. The network outputs were given in loss of the second moment of area, I (in %).

To assess the outcomes of the neural networks, the severity predictions were evaluated by normalised errors (NE_{sev}), which are defined as:

$$NE_{sev} = \frac{(T_d - O_d)}{S_{max}} \tag{2}$$

where d is the damage scenario, T_d the target value of d, O_d the network output value of d and S_{max} the maximum severity of damage (i.e. 100% loss of the second moment of area, I).

Results and Discussions

For the laboratory and numerical two-storey framed structure, neural networks were trained to identify severities of various damage scenarios. The outcomes of the networks are presented in the following sections by different tables and figures. The displayed tables list the performance of the trained networks, i.e. the 14 individual sensor networks trained with data from measurement locations ‘1’ to ‘14’, the two individual summation networks trained with data from horizontal and vertical summation FRFs (‘SumH’ and ‘SumV’) and the network ensemble (‘Ens’). The performance is given in absolute mean of normalised error (AMNE). The presented figures illustrate the network performance of the testing set outcomes subdivided by damage severity level.

Damage Identification of Laboratory Two-Storey Framed Structure

For the laboratory structure, network performance is given in Table 4 with detailed illustrations of the testing set outcomes displayed in Figure 8. From the network results, it is observed that among the

networks trained with horizontal acceleration data (networks ‘1’ to ‘8’), the networks of locations ‘1’ and ‘3’ perform the best with AMNE values of 0.02%. These outcomes are expected as locations ‘1’ and ‘3’ are the sites of the inflicted damage. The networks of locations ‘5’ and ‘7’ also give very good quantification outcomes with AMNE values of 0.26% and 0.54%. For the networks of locations ‘2’, ‘4’, ‘6’ and ‘8’, however, underperforming results are obtained with testing set AMNE values ranging from 3.50% to 5.19%. The reason for these larger errors is that vibrational data of measurement locations ‘2’, ‘4’, ‘6’ and ‘8’ have low sensitivity to local modes due to the fixity of the joint elements to the columns. Hence, the damage patterns in FRFs of these locations are limited and therefore lead to poorer severity identifications. For the networks trained with vertical data from the crossbeams (networks ‘9’ to ‘14’), very good outcomes are obtained with the networks of locations ‘9’ to ‘12’ achieving AMNE values from 0.02% to 0.10%. For the networks trained with data of locations ‘13’ and ‘14’, some light and medium damage cases are quantified with larger errors; good predictions are obtained for damage of light severity. For the horizontal and vertical summation networks as well as for the network ensemble, very good identification results are achieved. It is noted that the network ensemble outperforms the summation networks, which demonstrates the efficiency and importance of the ensemble approach that filters poor results from bad performing networks and gives better outcomes than any of the individual networks.

Table 4 Performance of networks trained with data of the laboratory structure to identify damage severities.

Net-work	Training performance (AMNE [%])	Validation performance (AMNE [%])	Testing performance (AMNE [%])
‘1’	0.01	0.31	0.02
‘2’	1.57	3.11	3.50
‘3’	0.01	0.02	0.02
‘4’	3.89	3.58	4.67
‘5’	0.01	0.15	0.26
‘6’	4.46	3.96	3.74
‘7’	0.01	1.27	0.54
‘8’	5.04	4.91	5.19
‘9’	0.03	0.08	0.03
‘10’	0.02	0.08	0.10
‘11’	0.01	0.02	0.02
‘12’	0.01	0.01	0.02
‘13’	0.26	0.91	1.12
‘14’	0.16	0.54	0.57
SumH	0.01	0.11	0.09
SumV	0.01	0.04	0.03
Ens	0.01	0.03	0.01

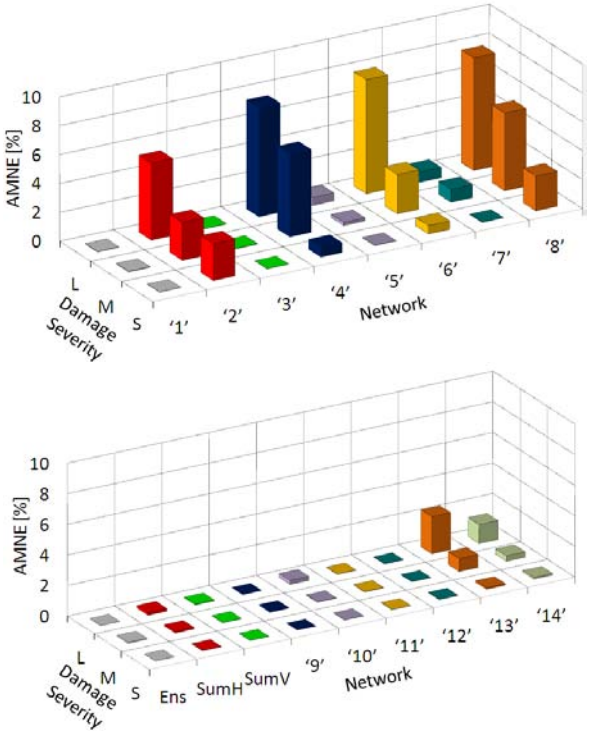

Figure 8 Testing set performance of networks trained with laboratory data to quantify damage subdivided by damage severities.

Damage Identification of Numerical Two-Storey Framed Structure

For the numerical simulations, Table 5 lists the performance of the networks. Illustrations of the testing set outcomes are shown in Figure 9. Again, the individual networks trained with data of locations ‘1’ and ‘3’ give the best outcomes, with AMNE values of only 0.11% and 0.46%, respectively. The networks of location ‘5’ and ‘7’ also perform well. Inferior damage quantifications are again obtained from the networks trained with data of locations ‘2’, ‘4’, ’6’ and ‘8’. For the networks trained with data derived

from vertical accelerations, reasonably good quantification outcomes are obtained. Good severity identification are also given by the networks trained with horizontal and vertical summation FRFs, with testing set AMNEs of 0.56% and 0.93%, respectively. With an AMNE of 0.04%, the network ensemble gives the best quantification outcomes among all networks. These results stress again the superiority of the network ensemble, which gives results that are better than the outcomes of any of the individual networks.

Table 5 Performance of networks trained with data of the numerical structure to identify damage severities.

Net-work	Training performance (AMNE [%])	Validation performance (AMNE [%])	Testing performance (AMNE [%])
'1'	0.02	0.14	0.11
'2'	1.17	1.21	1.20
'3'	0.11	0.37	0.50
'4'	2.38	2.86	2.90
'5'	0.74	1.12	1.17
'6'	3.57	4.49	4.45
'7'	1.21	1.63	1.72
'8'	2.11	2.88	2.80
'9'	1.18	1.48	1.39
'10'	1.24	1.23	1.28
'11'	2.16	2.53	2.73
'12'	2.06	2.61	2.63
'13'	0.36	0.37	0.36
'14'	2.11	2.35	2.36
SumH	0.41	0.53	0.56
SumV	0.59	1.02	0.93
Ens	0.01	0.09	0.04

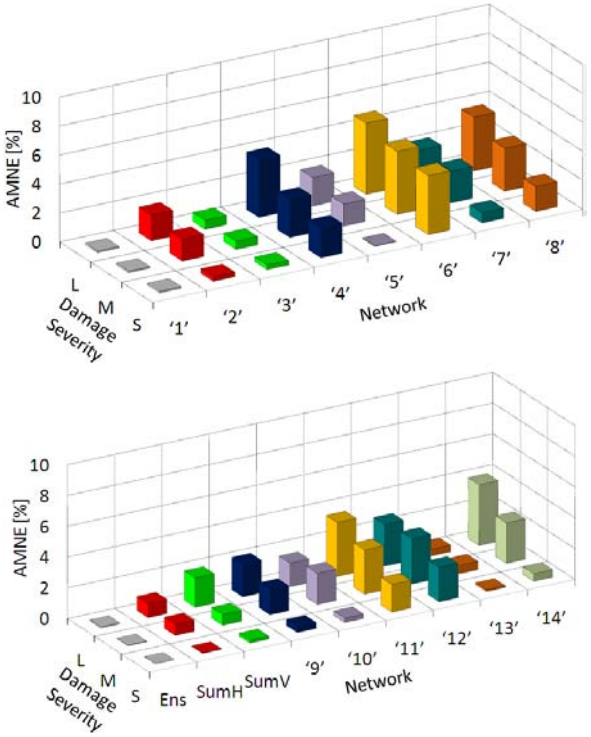

Figure 9 Testing set performance of networks trained with numerical data to quantify damage subdivided by damage severities.

Conclusions

This paper presented a vibration-based damage identification method to quantify notch-type damage in a numerical and laboratory two-storey framed structure. In the proposed method, damage fingerprints in FRF data in combination with ANN and PCA were utilised to identify severities of damage. For the laboratory and numerical structure, FRF data were determined at different locations of the structure by means of modal testing and transient analysis. To enhance embedded damage fingerprints in FRFs, residual FRFs, which are differences in FRF data between the undamaged and the damaged structure, were used as damage indicators. PCA techniques were adopted to extract damage features from residual FRFs, to compress the large size of measured FRF data and to remove noise. To take advantage of individual characteristics from FRFs of different measurement locations, a hierarchical neural network training based on network ensembles was implemented. In the network ensemble, first, a number of individual networks were trained with data separated by measurement location and then, the outcomes of the individual networks were fused in a network ensemble to give final damage predictions. Further, two additional individual neural networks were studied. These networks were trained with data from summarised FRFs, which were obtained by adding up the FRF data from all individual FRF measurements. White Gaussian noise of up to 10% noise-to-signal-ratio was added to numerical data to simulate field-testing conditions.

The damage identification results of both the laboratory and experimental structure showed that the proposed method is accurate and robust in the severity prediction of notch-type damage. For both types of the structure (numerical and experimental) the network ensembles gave precise identifications for all investigated damage cases. From the results, it was found that the proposed network ensemble approach was highly efficient in filtering bad estimation outcomes from poorly performing individual networks and achieving final ensemble outcomes that were generally better than the predictions of any of the individual networks. In addition, the network ensemble proved to be more accurate than the networks trained with data obtained from summation FRFs, which highlights the superiority of the network ensemble technique against the approach of simply summing FRF data from different measurement locations. The study further showed that it is crucial to capture FRF data from different locations of the structure, as at some locations, i.e. locations '2', '4', '6' and '8', FRF data turned out to have low sensitivity to local modes, resulting in error-prone damage identifications for networks trained with data of these locations. For the two-storey framed structure, ideal sensor placements were found to be the midpoints of the column halves (measuring horizontal acceleration) and any location on the crossbeams (measuring vertical acceleration).

Acknowledgements

The authors wish to thank the Centre for Built Infrastructure Research (CBIR), Faculty of Engineering and Information Technology, University of Technology Sydney (UTS) for supporting this project. Within the Faculty of Engineering, the authors wish to express their gratitude to the staff of UTS Structures Laboratory for their assistance in conducting the experimental works. Alyuda Research Inc. is gratefully acknowledged for providing a free copy of their Alyuda NeuroIntelligence software.

References

Alyuda Research Inc (2006), *Alyuda NeuroIntelligence*, version 2.2

ANSYS Inc (2007), *ANSYS*, release 11.0.

ANSYS Inc (2007), *ANSYS Workbench*, release 11.0.

CADA-X (1996). "Modal analysis manual", *LMS International*, Belgium.

Huynh, D., He, J. and Tran, D. (2005), "Damage location vector: a non-destructive structural damage detection technique", *Computers and Structures*. **83**(28-30), 2353-2367.

Levin, R.I. and Lieven, N.A.J. (1998), "Dynamic finite element model updating using neural networks", *Journal of Sound & Vibration*. **210**(5), 593-607.

Marwala, T. and Hunt, H.E.M. (1999), "Fault identification using finite element models and neural networks ", *Mechanical Systems and Signal Processing*. **13** 475-490.

Ni, Y.Q., Zhou, X.T. and Ko, J.M. (2006), "Experimental investigation of seismic damage identification using PCA-compressed frequency response functions and neural networks", *Journal of Sound and Vibration*. **290**(1-2), 242-263.

Wang, B.-s., Ni, Y.-q. and Ko, J.-m. (2000), "Influence of Measurement Errors on Structural Damage Identification using Artificial Neural Networks", *Journal of Zhejiang University SCIENCE* **1**(3), 291-299.

Zang, C. and Imregun, M. (2001), "Structural damage detection using artificial neural networks and measured FRF data reduced via principal component projection", *Journal of Sound and Vibration*. **242**(5), 813-827.